



Title	Elimination of hysteresis effect in superparamagnetic nanoparticle detection by GMR sensors for biosensing
Author(s)	Li, L; Lo, W; Leung, CW; Ng, S; Pong, PWT
Citation	The 2015 IEEE International Magnetics Conference (INTERMAG 2015), Beijing, China, 11-15 May 2015. In Conference Proceedings, 2015, paper no. CT-03
Issued Date	2015
URL	http://hdl.handle.net/10722/216416
Rights	IEEE International Magnetics Conference (INTERMAG). Copyright © IEEE.

Elimination of hysteresis effect in superparamagnetic nanoparticle detection by GMR sensors for biosensing.

L. LI¹, W. LO¹, C. LEUNG², S. NG², P. PONG¹

1. Department of Electrical and Electronic Engineering, The University of Hong Kong, Hong Kong; 2. Department of Applied Physics, Hong Kong Polytechnic University, Hong Kong

The biosensing methods utilizing superparamagnetic nanoparticles as bio-tags and giant magneto-resistive (GMR) or tunneling magnetoresistive (TMR) sensors as signal detectors have attracted increasing interests in early disease diagnosis as well as in molecular biology research area. [1] To achieve the signal of targets, one commonly used method is to compare the sensor hysteresis loops before and after the introducing of superparamagnetic nanoparticles onto sensor surface, and the sensor response variation has been regarded as an indicator of target analyte's amount. [2, 3] However, the hysteresis effect existing in ferromagnetic material may bring an error in the sensor output reading, which can be problematic in the superparamagnetic nanoparticle signal detection. Since the hysteresis behavior exists in all magnetoresistive sensors made of ferromagnetic material, it is necessary to investigate its effect on superparamagnetic nanoparticle detection and eliminate its negative influences.

In this work, we developed a robust measurement protocol based on GMR sensor in Wheatstone bridge to suppress the signal error caused by hysteresis effect, and demonstrated its ability to detect 20-nm carboxyl group functionalized superparamagnetic nanoparticles. The GMR sensor in Wheatstone bridge used here consists of a seed layer, antiferromagnetic layer, synthetic antiferromagnetic layer, spacer, free layer, and top layer (Fig. 1a). 20-nm carboxylate superparamagnetic iron oxide nanoparticles (Inset in Fig. 1a) were used here to test the detection ability of GMR sensor. There are four elements in a Wheatstone bridge configuration (Fig. 1b). R_1 and R_3 serve as sensing elements and R_2 and R_4 serve as compensating elements. In our measuring setup, the Helmholtz coils provided an in-plane magnetic field. A DC current of 1×10^{-4} A was applied to the Wheatstone bridge for output voltage measurements, and thus its output signal was designated as delta resistance ($\Delta R = V_{Out}/I_{In}$). The ΔR of the GMR sensor changed with applied magnetic field along its easy axis. The hysteresis loop of GMR sensor (Fig. 1c) displayed typical hysteresis effect, which was magnified as the inset shows. Here, the sensor hysteresis loop was measured versus magnetic field repeatedly to make the magnetic history of sensor towards to be constant. To suppress the error origins from the intrinsic defect in the GMR sensor during the course of magnetization reversal, the sensor output resistance values from ten hysteresis loops were averaged to get an $M-R_{ave}$ loop with averaged R value for every magnetic field point. When introducing the superparamagnetic nanoparticles onto sensor surface, the nanoparticles were magnetized by the applied magnetic field and the in-plane component of the stray field emanated from the nanoparticles caused additional variation of ΔR compared with control sensor. The signal curve was fitted by Gauss function to get its peak point value as the nanoparticles signal. A flowchart of our measurement procedure for the detection of superparamagnetic nanoparticles by GMR sensor is illustrated in Fig. 2a. Our results indicate that the resistance error was suppressed from 9.9 Oe (Fig. 2b1) to 2.5 Oe (Fig. 2b2) by utilizing $M-R_{ave}$ loops. After introducing the 20-nm carboxylated superparamagnetic nanoparticles onto GMR sensor surface, the typical relation of ΔR variation against easy-axis applied magnetic field is shown in Fig. 2c. The signal curve was fitted by Gauss function to obtain the nanoparticles signal, and the signals incurred by superparamagnetic nanoparticles with thirteen concentrations on GMR sensor were plotted in Fig. 2d. The signal of deionized water serves as the control one. Here, the final signal values for the nanoparticles with concentrations of 10 ng/ml, 100 ng/ml and 1 μ g/ml were comparable with the baseline of 2.5 Ω , and the signal for nanoparticles with concentrations of 3 mg/ml, 3.5 mg/ml and 4 mg/ml were at saturated plateau of 77 Oe. The signals for nanoparticles with detectable concentrations were 5.2 Ω (10 μ g/ml), 5.8 Ω (100 μ g/ml), 14.4 Ω (500 μ g/ml), 22.6 Ω (1 mg/ml), 35.6 Ω (1.5 mg/ml), 70.0 Ω (2 mg/ml) and 75.3 Ω (2.5 mg/ml). In summary, a robust measurement procedure to eliminate the hysteresis effect in superparamagnetic nanoparticle detection by GMR sensor was established, and its detection ability of superparamagnetic nanoparticles was demonstrated.

- [1] L. Li, C. Leung, and P. Pong, "Magnetism of Iron Oxide Nanoparticles and Magnetic Biodetection," *Journal of Nanoelectronics and Optoelectronics*, vol. 8, pp. 397-414, 2013.
 [2] G. Li, S. Sun, R. J. Wilson, R. L. White, N. Pourmand, and S. X. Wang, "Spin valve sensors for ultrasensitive detection of superparamagnetic nanoparticles for biological applications," *Sensors and Actuators A: Physical*, vol. 126, pp. 98-106, 2006.
 [3] W. Shen, B. D. Schrag, M. J. Carter, J. Xie, C. Xu, S. Sun, et al., "Detection of DNA labeled with magnetic nanoparticles using MgO-based magnetic tunnel junction sensors," *Journal of Applied Physics*, vol. 103, pp. 07A306-3, 2008.

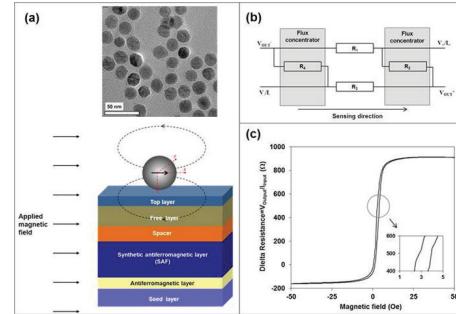


Figure 1. (a) Illustration of superparamagnetic nanoparticle detection using GMR sensor in in-plane mode. Inset: TEM image of 20-nm carboxylate magnetic iron oxide nanoparticles. (b) Layout of a GMR detector. R_1 and R_3 serve as sensing elements and R_2 and R_4 serve as compensating elements. (c) Transfer curve of the GMR sensor in Wheatstone bridge. Magnified part in inset shows typical hysteresis effect.

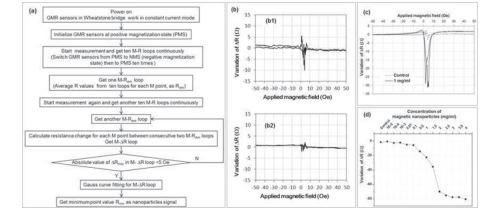


Figure 2. (a) Flowchart of optimized measurement procedure for the detection of superparamagnetic nanoparticles. (b) Error from hysteresis effect in GMR sensor was suppressed from (b1) 9.9 Ω to (b2) 2.5 Ω by utilizing $M-R_{ave}$ loops. (c) Relation of ΔR variation for deionized water (control – dashed line) and superparamagnetic nanoparticles (1 mg/ml – solid line) against easy-axis applied magnetic field. (d) Signals obtained for superparamagnetic nanoparticle with thirteen different concentrations.